Non-linearity analysis of a spectroradiometer

K. Torgasin[a] and A. Baumgartner[a]

[a]German Aerospace Center (DLR), Münchner Straße 20, Oberpfaffenhofen, Germany

ABSTRACT

Hyperspectral analysis is an important remote sensing tool. Corresponding spectrometers require accurate calibration in optical laboratories. Non-linearity and temperature dependence are important factors that degrade the calibration quality. In this paper, we report on the investigation of the non-linearity of a temperature stabilized spectroradiometer *HR-1024i* from Spectra Vista Corporation (SVC). The spectroradiometer is applied as transfer spectroradiometer for the radiometric calibration of air- and spaceborne imaging spectrometers. Results show signal dependent non-linearity. The non-linearity of the spectrometer's *VNIR* detector in spectral range $450 - 980\,nm$ shows a strong spectral channel dependence with maximal radiometric error of 2%. The non-linearity of the *SWIR-2* detector in spectral range $1896 - 2510\,nm$ could not be evaluated precisely due to the low signal level. This impact of non-linearity requires correction in post-data processing.

Keywords: transfer radiometer, remote sensing, calibration, non-linearity

1. INTRODUCTION

Spectroradiometers are applied in remote sensing for the validation of ground radiance measured by airborne or spaceborne detectors.[1] For that reason, the radiometer has to be characterized and calibrated in an optical laboratory. The Calibration Home Base (CHB)[2] of the Remote Sensing Technology Institute (IMF) at the German Aerospace Center (DLR) uses a Spectra Vista Corporation (SVC) *HR-1024i* spectroradiometer for the radiometric calibration of several hyperspectral imaging systems such as the Airborne Prism Experiment (APEX),[3] the Munich Aerosol Cloud Scanner (specMACS)[4] and the Environmental Mapping and Analysis Program (EnMAP).[5]

The main application of a transfer spectroradiometer is the transfer of radiance responsivity, measured at standard radiance source at a certain temperature, to an integration sphere, which is used as radiance calibration source for an imaging spectrometer under test. Usually the radiance is measured at certain level and linearly extrapolated to full dynamic range of the transfer spectroradiometer. Hence, non-linearity (NL) can have a significant impact on the radiometric accuracy. The NL is understood as deviation from linear correlation between the detected signal and the incident light intensity. The deviation can be classified in integration time dependent NL and signal dependent NL or combination of both. In case of integration time dependence, the NL is attributed to the difference between the set and the actual integration time. The second case refers to errors in charge collecting and signal converting electronics, respectively.[6,7]

There are several methods to measure NL, like double aperture- and multi-distance methods.[8,9] Hereby the basic idea concerns variation of at-aperture radiance preferably over the full dynamic range of the sensor.[10] Any deviation from the ideal linear line of the acquired signal as function of radiance corresponds to NL.

The NL of a SVC *HR-1024i* spectroradiometer has been characterized previously.[11] This report concerns an upgraded model with a thermally stabilized Visible to Near InfraRed (*VNIR*) detector measuring in the range $341 - 1010\,nm$. The upgrade reduces the dependence of the radiometric response on environmental temperature. For our purposes the uncertainty due to the NL has to be $\leqslant 0.1\%$. Hence, the objectives of this work is to estimate the NL of the upgraded spectroradiometer.

Further author information: (Send correspondence to Konstantin Torgasin)
Konstantin Torgasin: E-mail: konstantin.torgasin@dlr.de, Telephone: +49(0)8153281129

SPIE Future Sensing Technologies 2024, edited by Osamu Matoba, Joseph A. Shaw, Christopher R. Valenta, Proc. of SPIE Vol. 13083, 130831D · © 2024 SPIE
0277-786X · doi: 10.1117/12.3023000

2. MATERIALS AND METHODS

2.1 Instrumentation

The SVC *HR-1024i* spectroradiometer is measuring radiance simultaneously by three CCD arrays, covering Visible to Near InfraRed (*VNIR*) in $341 - 1010\,nm$), Short-Wave InfraRed (*SWIR-1*) in $974 - 1910\,nm$ and *SWIR-2* in $1899-2515\,nm$ spectral ranges. Table 1 summarizes the main characteristics of the spectroradiometer. Further properties can be found on web-page of the manufacturer.[12]

Table 1: Detector arrays characteristics of the SVC *HR-1024i* spectroradiometer used in this work.

Detector	Spectral range	Channels	Temperature	Integration time (step size)
VNIR (Si)	341 - 1010 nm	512	- 9° C	1 - 100 ms (10)
SWIR-1 (InGaAs)	974 - 1910 nm	256	- 5° C	1 - 50 ms (1)
Swir-2 (extended InGaAs)	1899- 2515 nm	256	- 10° C	1- 20 ms (1)

2.2 Setup

Figure 1 shows a schematic drawing of the experimental setup. A Quartz Tungsten Halogen (QTH) lamp ($1\,kW$) is connected to an integration sphere. The radiance coming from an output port of the integration sphere is coupled to a $1\,m$ long fiber optic bundle, which is connected to the spectroradiometer (*HR-1024i*). Another output port is connected by an optical fiber to a radiometer (*Gamma Scientific*, 19830−4) for radiometric stability control. The spectroradiometer as well as the QTH lamp were warmed up for 1 hour prior to measurement.

In order to acquire data of various signal levels over whole dynamic range, two methods were combined. The radiance level was adjusted by lamp power. Additionally for each radiance level the integration time was varied. Data analysis demonstrates that signals obtained by both methods can be evaluated together.

The spectra over the full spectral range is measured five times with 100 different integration time (τ_{int}) settings. For all three detectors there is separate time setting (see Tab. 1). The integration time at each record was randomly set in order to avoid systematic errors due to lamp or instrument drift. Finally, the data was averaged over five measurements with the same τ_{int} settings. The respective dark signal was automatically recorded after each measurement using the spectrometer's internal shutter.

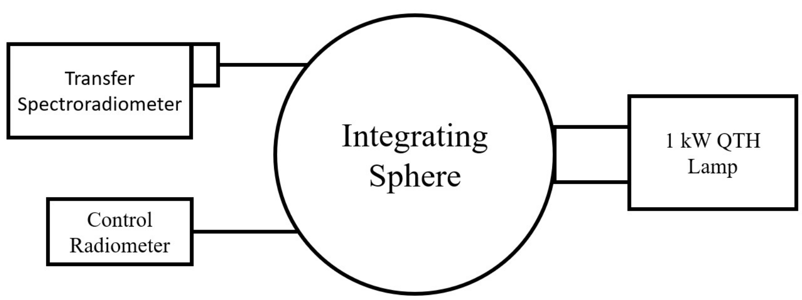

Figure 1: Experimental setup for the measurement of non-linearity at various integration times and radiation levels.

2.3 Data processing

An example of recorded spectra at various τ_{int} is shown in Fig. 2. It can be seen that the sensibility of each detector is declining around the edge regions. The detectors *VNIR* and *SWIR-1* are saturated at longer integration times. Saturation levels correspond to >30180 digital numbers (DN) (*VNIR*) and $>21400\,DN$ (*SWIR-1*). The saturated data were disregarded for analysis. The signal level for the *SWIR-2* detector is low $<10000\,DN$, and is therefore not saturated.

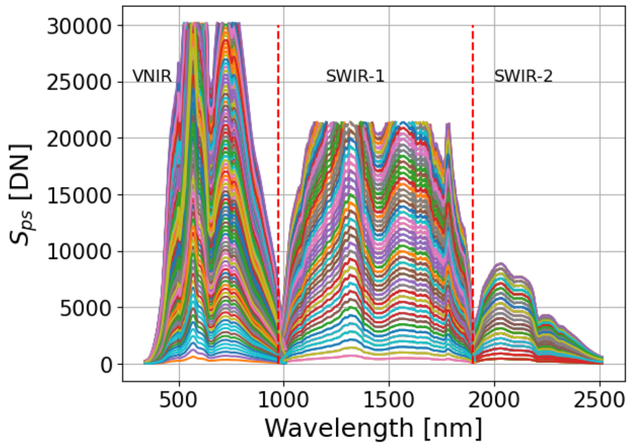

Figure 2: Signal recorded by the 3 detectors with varying integration times. The red dashed lines indicate edges of detectors. The spectra show saturation above 30180 DN for *VNIR*, above 21400 DN for *SWIR-1* and no saturation for *SWIR-2*.

A linear detector measures a signal consisting of photo signal S_p, dark signal S_d and an electronic offset S_{off}. The photo signal is generated by incident photons, whereas the dark signal is caused mainly by thermally generated electron hole pairs. Since we are interested in the amount of measured photons, the offset has to be subtracted from the total signal. The offset is determined as fitting parameter from linear fit of the dark signal vs. integration time over the 10 lowest integration time settings. Figure 3 shows corresponding dark signal for 3 spectral channels as measured with closed shutter.
The offset S_{off} for all three detectors (*VNIR*, *SWIR-1*, *SWIR-2*) is shown in Fig. 4. According to these results the detectors *SWIR-1* and *SWIR-2* have a high dark signal and noise level, respectively.
The acquired signal is corrected for offset according to equation:

$$S_{corr} = S_p + (S_d - S_{off}) \,. \tag{1}$$

For the NL evaluation, the corrected signal S_{corr} is divided by integration time τ_{int} and normalized by quotient's mean value:

$$S_{norm} = \frac{S_{corr}}{\tau_{int}} / \left\langle \frac{S_{corr}}{\tau_{int}} \right\rangle \,. \tag{2}$$

In an ideal linear case the plot of S_{norm} vs. S_{corr} results in a line with the slope = 1.

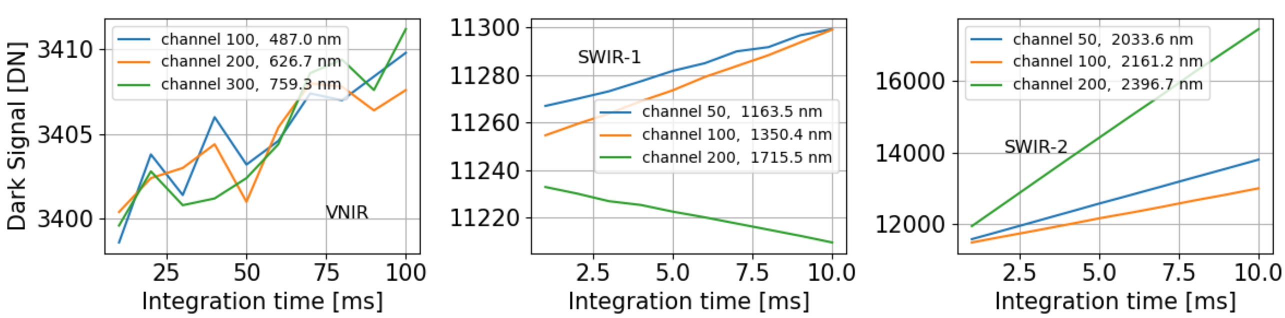

Figure 3: Determination of signal offset for the three detectors - *VNIR*, *SWIR-1*, *SWIR-2*. The integration time dependence of the dark signal is plotted for the 10 smallest integration times for 3 spectral channels.

In order to cover full dynamic range of the sensor, data from different series of measurements were merged. Figure 5a shows overlay plots of 4 data sets for the spectral channels 100, 200 and 300 of the *VNIR* detector.

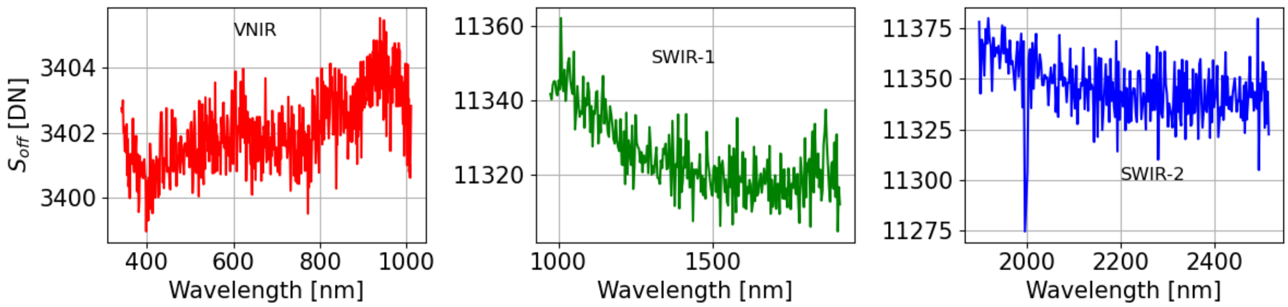

Figure 4: Signal offsets for the three detectors - *VNIR*, *SWIR-1*, *SWIR-2*. The offset is obtained as fitting parameter from linear fit of plots from Fig. 3.

The merged data for the same channels are plotted in the Fig. 5b. A linear fit allows us to estimate the NL as deviation from a constant value of S_{norm}.
Similar analysis was performed for detectors *SWIR-1* and *SWIR-2* as shown in Figures 6a, 6b, 6c, 6d.

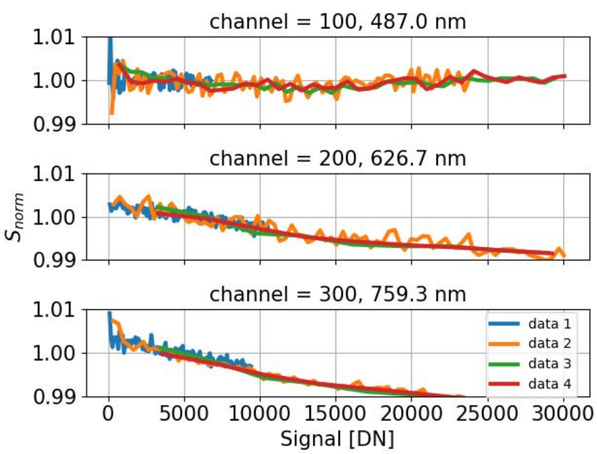

(a) Data from different measurements overlayed

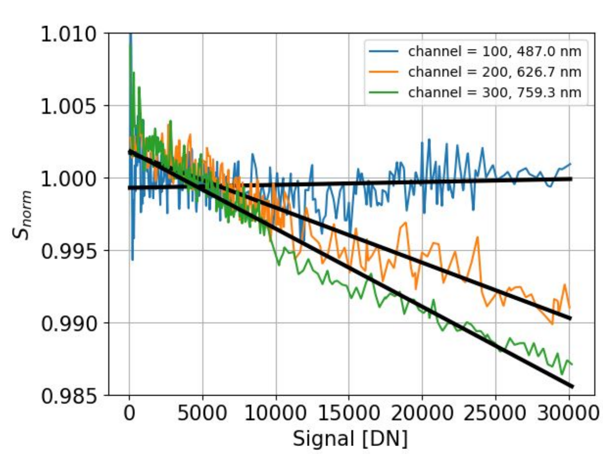

(b) Merged and interpolated data

Figure 5: Overlayed and merged data sets of *VNIR* detector, plotted for spectral channels 100, 200 and 300. The merged data are fitted with linear regression. The resulting slopes correspond to non-linearity.

3. RESULTS

The slope of the line fit, as described in previous subsection, corresponds to the maximum error due to NL. The maximum error due to the NL in percent, as derived from the fit for all three detectors, is shown in Fig. 7. However, the fit itself has uncertainties attributed to the data quality. Data sets with low signal levels induce noise, diminishing the fit quality. Detector edge regions have increased noise levels due to the lower sensitivity. The fit is evaluated by the standard deviation of the residuals, as shown in subplots of Fig. 7.
The *VNIR* detector shows channel dependent NL with a maximum radiometric error of 2%. The signal level below 10000 DN has high noise influence. Thus, fits with a standard deviation of residuals above 0.003 are disregarded and not shown in Fig. 7. The *SWIR-2* detector shows in general low signal level ($<$10000 DN). The signal level below 3000 DN shows a positive slope, for signals above this value the slope is negative, see Fig. 6c. This behavior results in higher fit uncertainties. The resulting estimation of NL has a spread over 1%, as shown in Fig. 6d. The *SWIR-1* has a desired NL below 0.1% with slight rise in at the edge regions.

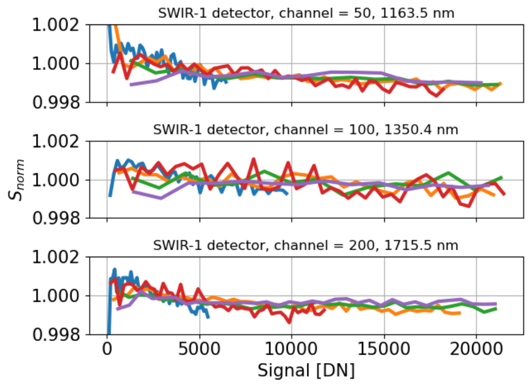

(a) Data sets for *SWIR-1*

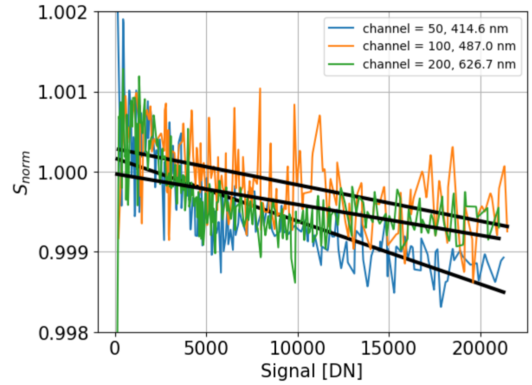

(b) Merged and interpolated data for *SWIR-1*

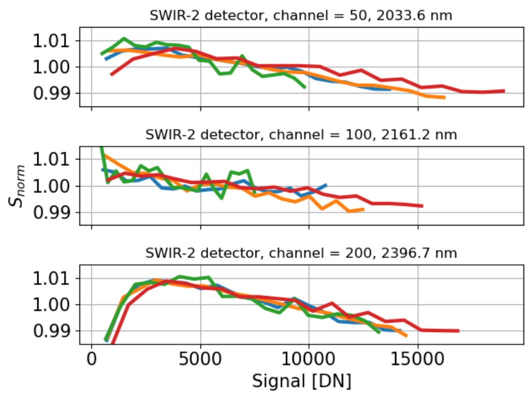

(c) Data sets for *SWIR-2*

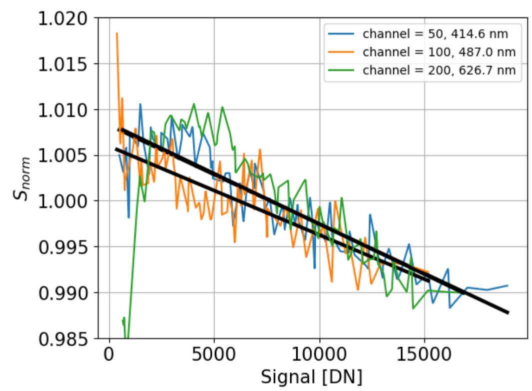

(d) Merged and interpolated data for *SWIR-2*

Figure 6: Ovelayed and merged data sets for *VNIR*, *SWIR-1* and *SWIR-2* detectors, plotted for 3 spectral channels. The merged data are fitted with linear regression. The maximal non-linearity is derived from resulting slopes.

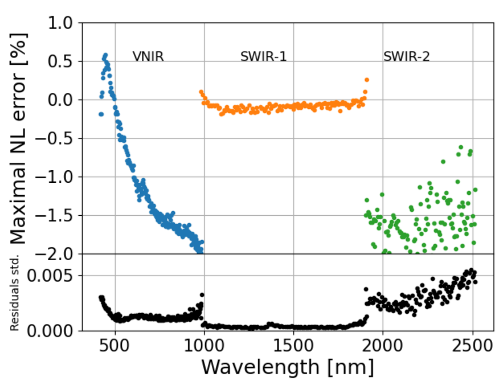

Figure 7: Non-linearity of the three detectors as function of spectral channels.

4. DISCUSSION AND CONCLUSIONS

In this paper, we have reported the investigation of the non-linearity of temperature stabilized *HR-1024i* spectroradiometer from Spectral Vision Corporation. For that reason we have combined two methods. Variation of radiation level by power of the light source, whereby at each radiation level signal with different integration time settings was measured. The non-linearity was derived from the linear fit of normalized data over several signal

levels for each spectral channel. The results show similar dependence of detected signal level on integration time for different measurement series. This is an indication for linearity of the integration time setting. Hence the observed non-linearity depends on the signal level.
The data with low signal levels, especially of the detector edge regions, have high noise, so that the non-linearity cannot be analyzed precisely. In order to reduce this drawback, the measurement setup has to be modified to increase illumination at those regions.
The non-linearity of the detector *VNIR* is strongly channel dependent with maximum deviation of 2%. The noise at the edge regions has a strong impact for this detector. The *SWIR-2* detector has high uncertainty for determination of non-linearity due to the low signal level. The estimation of non-linearity by linear fit is not proper method at such low signal levels. Since our target value for detectors non-linearity is $\leqslant 0.1\%$, a correction has to be applied to the data obtained from the *VNIR* and *SWIR-2*. The non-linearity of the *SWIR-1* detector corresponds to the desired value without need for correction.

REFERENCES

[1] Schaepmann, W. E. and Dangel, S., "Solid laboratory calibration of a nonimaging spectroradiometer," *Appl. Opt.* **39**, 3754–3764 (2000).

[2] 'DLR Remote Sensing Technology Institutel', "Solid laboratory calibration of a nonimaging spectroradiometer," *JLSRF* **2, A82**, 1–9 (2016).

[3] Schaepman, M. E., Jehle, M., Hueni, A., D'Odorico, P., Damm, A., Weyermann, J., Schneider, F. D., Laurent, V., Popp, C., Seidel, F. C., Lenhard, K., Gege, P., Küchler, C., Brazile, J., Kohler, P., De Vos, L., Meuleman, K., Meynart, R., Schläpfer, D., Kneubühler, M., and Itten, K. I., "Advanced radiometry measurements and earth science applications with the airborne prism experiment (apex)," *Remote Sens. Environ.* **158**, 207–219 (2014).

[4] Ewald, F., Kölling, T., Baumgartner, A., Zinner, T., and Mayer, B., "Design and characterization of specmacs, a multipurpose hyperspectral cloud and sky imager," *Atmos. Meas. Tech.* **9**, 2015–2042 (2016).

[5] Polz, L., Serdyuchenko, A., Lettner, M., Mücke, M., and Fischer, S., "Setups for alignment and on-ground calibration and characterization of the enmap hyperspectral imager," *Proc. of SPIE* **11852**, 118526B–1 – 118526B–14 (2021).

[6] Pulli, T., Nevas, S., Gawhary, O. E., van den Berg, S., Askola, J., Kärhä, P., Manoocheri, F., and Ikonen, E., "Nonlinearity characterization of array spectrometers for the solar uv measurements," *Appl. Opt.* **56**, 3077–3086 (2017).

[7] Nehir, M., Frank, C., Aßmann, S., and Achterberg, P., "Improving optical measurements: non-linearity compensation of compact charge-coupled device (ccd) spectrometers," *Sensors* **19, 2833**, 1–16 (2019).

[8] Talone, M., Zibordi, G., and Białek, A., "Reduction of non-linearity effects for a class of hyper-spectral radiometers," *Metrologia* **57, 025008**, 1–7 (2020).

[9] Salim, S. G. R., Fox, N. P., Theocharous, E., Sun, T., and Grattan, K. T. V., "Temperature and nonlinearity corrections for a photodiode array spectrometer used in the field," *Appl. Opt.* **50**, 866–875 (2011).

[10] Nevas, S., Teuber, A., Sperling, A., and Lindemann, M., "Stability of array spectroradiometers and their suitability for absolute calibration," *Metrologia* **49**, 48–52 (2012).

[11] Rammeloo, C. and Baumgartner, A., "Spectroradiometer calibration for radiance transfer measurements," *Sensors* **23, 2339**, 1–13 (2023).

[12] Spectra Vista Corporation, "Homepage." https://spectravista.com/instruments/hr-1024i/. (Accessed: 4 April 2024).